ORGANIC SONOELECTROCHEMISTRY ON MERCURY POOL ELECTRODE

Jiří KLÍMA[1,*] and Jiří LUDVÍK[2]
J. Heyrovský Institute of Physical Chemistry, Academy of Sciences of the Czech Republic,
Dolejškova 3, 182 23 Prague, Czech Republic; e-mail: [1] klima@jh-inst.cas.cz,
[2] ludvik@jh-inst.cas.cz

Received January 14, 2000
Accepted March 22, 2000

Presented at the 32nd Heyrovský Discussion on Organic Electrochemistry, Třešť, June 6–10, 1999.

So far, the influence of sonication on the electrolytic current was studied only at solid or rather miniaturized mercury electrodes. The presented paper reports on sonoelectrochemical experiments at a liquid mercury pool electrode. Two sonoelectrochemical cells have been developed and tested. It was shown that during sonication, the electrolytic current increases in a number of individual peaks representing short local enhancements of current density due to vigorous local mass transfer and instantaneous increase of fresh electrode surface. Both these effects are caused by microjets of solution formed during violent unsymmetric collapses of cavitation bubbles in the close vicinity of the electrode surface. The newly formed electrode surface and the decrease in the diffusion layer thickness were estimated and discussed. An example is presented where the sonication is used for destruction of a film of products formed during electrolysis of cysteine, that otherwise rapidly inhibits continuation of the electrode process.

Key words: Sonoelectrochemistry; Ultrasound; Cavitation; Mercury pool electrode; Electrode activation; Electrochemistry; Electrolysis.

Sonoelectrochemistry is a technique which takes advantage of application of ultrasound in electrochemistry[1,2]. Sonication of working electrode or, more specifically, irradiation of the vicinity of the working electrode by power ultrasound results in three effects important from the point of view of electrochemistry:

1) *Acoustic streaming* which is a consequence of absorption of the ultrasonic energy. When some energy passing through a medium is absorbed, a pressure (called acoustic pressure in the case of ultrasonic energy) arises, acting on this medium. Such pressure can induce a macroscopic flow of solution[3,4]. This convective motion reduces the diffusion layer thickness, *i.e.*, increases mass transfer to the electrode and, consequently, enhances the electrochemical current[5]. The current density is fairly homogeneous over the electrode surface. The acoustic streaming depends on distribution of acoustic intensity and on the cell shape. As the acoustic pressure is proportional to the amount of the absorbed ultrasonic energy, the increase in current is approximately proportional to the acoustic power introduced to the cell.

2) *Microstreaming and turbulence* which result from cavitation, *i.e.*, formation, oscillation and collapse of small bubbles in solution[4,6]. Also, this motion causes a decrease in the diffusion layer thickness and enhancement of the mass transfer.

3) *Formation of microjets*; when a bubble collapses in the vicinity of a solid boundary (*e.g.*, electrode surface in the case of sonoelectrochemistry), a microjet of liquid is formed which beats the surface with high velocity[7]. Every jet transfers an amount of new solution containing starting molecules through the diffusion layer to a certain point of the electrode surface[8]. This type of mass transfer results in a fast local increase in current density followed by its slower decrease. The current density is inhomogeneous in both time and space dimensions. The electrochemical current increases in the form of a number of individual peaks[9]. Moreover, due to pulses of high pressure, which are formed when jets impact the surface ("liquid hammer pressure"), the surface of electrode may be changed[10–12]. Sonication can thus activate (depassivate) the electrode[13–15] by cleaning up its surface from passivating products, or even enlarge its surface by increasing roughness due to its erosion[16]. The sonochemical effect of microjets depends on the size and number of cavitating bubbles in the vicinity of the electrode surface, *i.e.*, on the local intensity of ultrasound in the closest electrode neighbourhood.

The local mass transfer enhancement and modification (activation) of the electrode surface by microjets is not only capable of increasing the rate of electrolysis[13], it may also improve current efficiency[17] and/or change the relative composition of a product mixture[18,19].

As the sonication is associated with a very intense motion of solution, solid electrodes have been used in absolute majority of sonoelectrochemical experiments. Mercury is a very suitable electrode material due to its high overvoltage of hydrogen evolution and a fairly defined and smooth surface. In the only reported sonoelectrochemical investigations with a liquid mercury working electrode[20,21] a low-intensity ultrasound was used, where the formation of microjets was very limited (or impossible). So far, a working electrode realized by liquid mercury has not been used in combination with power ultrasound. Attempts were made to use electrodeposited mercury film on platinum[22], copper and glassy carbon[23,24]; however, when high-intensity ultrasound is applied, an intense cavitation in the vicinity of the electrode results in ablation of the mercury film from the electrode surface[23,25].

The aim of this contribution is to show that advantages of sonication, *i.e.*, mass transfer enhancement and electrode surface activation, can be utilized even in the case when a liquid mercury pool electrode is used and power ultrasound is applied. A mechanism of the effects is proposed and discussed.

EXPERIMENTAL

Distilled water, acetonitrile for HPLC (Carlo Erba), electrochemical grade tetrabutylammonium hexafluorophosphate (TBAH, Fluka), KCl, $KClO_4$, Na_2SO_4 and $TlNO_3$ (all Merck) were used without further purification.

Potential control was achieved with a PAR Model 273A potentiostat or an AFCBP1 bipotentiostat (Pine Instrument Company).

An ultrasonic generator SON 200 working at 20 kHz frequency with maximum output 200 W and a sonicator with a piezoelectric transducer and a titanium horn (horn tip diameter 14 mm), both from EL-MEDICA (Kladno, Czech Republic) served as a source of ultrasound.

Two types of experimental arrangement were designed:

1) An arrangement with the ultrasonic horn immersed directly into an undivided electrochemical cell is depicted in Fig. 1a. The surface of mercury at the conically extended end of a glass tube (diameter 1 mm) served as a working electrode (surface area *ca* 16 mm^2). For experiments at the platinum working electrode, a platinum disc (surface area 0.2 mm^2) with vertical orientation was used. A platinum wire was employed as an auxiliary electrode. A

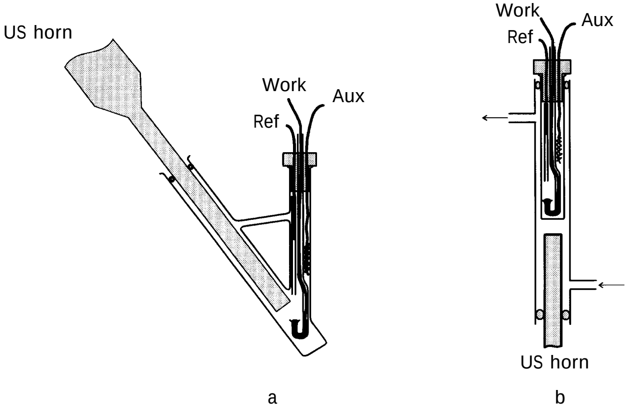

FIG. 1
Sonoelectrochemical cells: a cell with an ultrasonic horn immersed directly into the electrolyzed solution; b cell with the horn isolated from the electrolyzed solution by a glass wall

silver-wire quasi-reference electrode was placed near the surface of the solution where the intensity of ultrasound is low. The whole electrochemical cell was immersed into a bath thermostated to 293 K. The metallic tip of the horn connected to the ground is in contact with the solution. In order to avoid electrolysis at its surface, a four-electrode potentiostat is required[26]. As additional complication, most ultrasonic energy is absorbed directly near the surface of the horn, *i.e.*, in the cell. Consequently, the solution becomes rapidly heated when sonication is switched on (heating rate was *ca* 0.6 $K\ s^{-1}$ when the power output was set at 50 W). Regardless the cell was well thermostated, the temperature inside was not stable and increased by *ca* 4 K.

The advantage of this cell is the possibility to place the working electrode near the surface of the horn where the intensity of ultrasound is high. On the other hand, one should keep in mind that the intensity is distributed very inhomogeneously and decreases rapidly with increasing the horn-electrode distance.

2) The second arrangement, having the ultrasonic horn separated from the studied solution (Fig. 1b), is a modified version of the cell described in our previous paper[12]. An undivided electrochemical cell of a cylindrical shape (e.d. 15 mm, i.d. 12.5 mm) is immersed into a larger glass tube (i.d. 18.5 mm). A titanium horn with a tip area of 1.54 cm^2 is situated at the bottom of this tube. Water flowing through this tube serves both as a cooling agent and a coupling medium for transfer of ultrasonic energy from the horn to the cell. An overpressure of 0.2 to 0.3 MPa was kept in the cooling water in order to decrease the transient cavitation intensity outside the electrochemical cell. Depression of the transient cavitation outside the cell improves the coupling between the horn and water, *i.e.*, it reduces the absorption of ultrasound in the cooling water, hence improving the transfer of ultrasonic energy from the horn to the electrochemical cell.

The power input of ultrasonic energy to the electrochemical cell was determined calorimetrically[9]. In the case of the arrangement with the unseparated horn, all ultrasonic energy is transferred directly into the electrochemical cell. However, its large part converts into heat immediately at the horn-solution interface where the most intense cavitation takes place, and it does not reach the electrode surface.

In the second arrangement, the amount of the ultrasonic energy transferred into the electrochemical cell depends on the overpressure in the cooling medium. Without overpressure, a limited energy input of *ca* 0.6 W was obtained, which corresponds to an acoustic intensity of 0.5 $W\ cm^{-2}$ (the cross-section of the cell is 1.23 cm^2). With 0.3 MPa overpressure in the water cooling system the energy input increased up to *ca* 3.2 W and the acoustic intensity to 2.6 $W\ cm^{-2}$. Two principal advantages result from the second arrangement: (i) the horn is electrically isolated from the electrolyzed solution, and (ii) due to the cylindrical shape of the whole assembly, all the acoustic energy is passing through a constant area of *ca* 4 cm^2 (not increasing with the increasing distance from the horn). Consequently, the acoustic intensity does not rapidly diminish with distance, as it is the case of all directional spreading (in the latter case, the decrease in intensity approaches $1/r^2$ when the distance r is large compared to the horn radius).

RESULTS AND DISCUSSION

Results obtained with the arrangement according to Fig. 1b are presented in Figs 2–11, as the latter gives slightly better signal-to-noise ratio.

Charging and Faraday Currents on Mercury During Sonication

In the initial experiments, it was necessary to check the behaviour of the liquid mercury surface during sonication in both the types of cells. It was found that the mercury electrode is stable and does not for example disintegrate to small droplets.

Figure 2 presents blank current at a mercury pool electrode (0.1 M Na_2SO_4 in water) with and without sonication. A noise-like increase in current, *i.e.*, formation of a number of current peaks due to sonication, is observed. Figure 3 depicts the shape of an individual peak recorded at a higher time resolution.

Figure 4 presents voltammograms for aqueous solution of Tl^+ (0.5 mM $TlNO_3$, 0.1 M $KClO_4$) recorded at a mercury pool electrode. Again, sonication results in an increase in current in the whole potential range in a number of peaks. The shape of an individual pulse recorded at the reduction potential of Tl^+ is shown in Fig. 5.

In order to compare the results for the mercury pool with those obtained at solid electrodes, voltammograms recorded with a small (0.2 mm^2) platinum disk electrode are presented. A detailed analysis of the process has been published elsewhere[8,9]. Figure 6 shows voltammetric curves at the platinum electrode recorded in blank (0.1 M Na_2SO_4 in water) with and without sonication; Fig. 7 presents voltammograms of 0.23 mM methylviologen in aqueous solution. The shape of an individual current peak recorded for the same solution at *ca* –1.0 V is shown in Fig. 8.

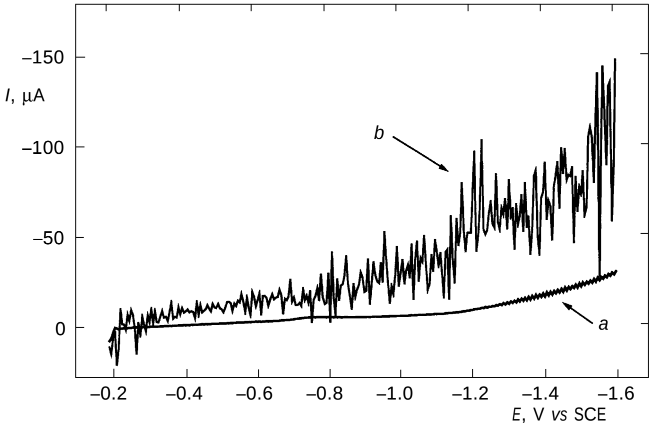

FIG. 2

Voltammograms recorded at a mercury pool electrode (surface *ca* 16 mm^2) in aqueous solution of supporting electrolyte (0.1 M Na_2SO_4): *a* without sonication; *b* with sonication. Scan rate 0.1 V s^{-1}

There are two most significant differences between the results at the liquid mercury electrode and the solid platinum electrode:

1) At the platinum electrode, there is no or negligible influence of sonication on the blank (charging) current, *i.e.*, on the current at the potential where none of the compounds present in the solution is electrochemically active. In the case of the mercury electrode, the current increases in a

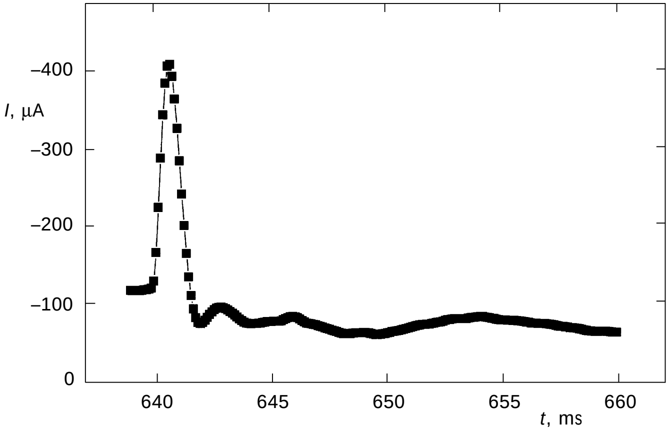

FIG. 3

Shape of an individual current peak at E = –0.98 V (*vs* SCE) recorded at higher time resolution (0.1 ms per point) at mercury pool electrode (0.1 M Na_2SO_4 in water)

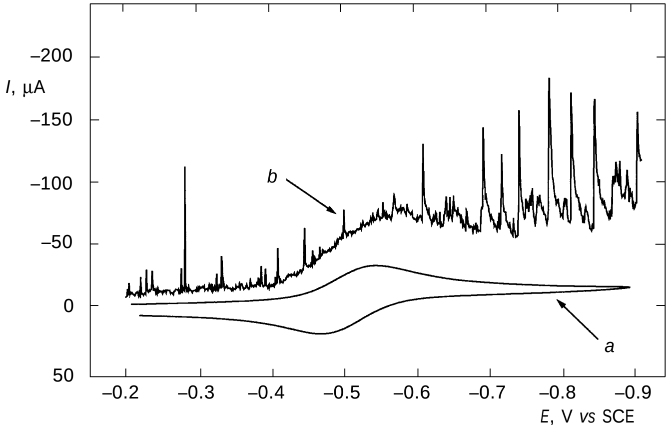

FIG. 4

Voltammograms recorded at mercury pool electrode (surface *ca* 16 mm^2) in aqueous solution of Tl^+ (0.5 mM $TlNO_3$, 0.1 M $KClO_4$): *a* without sonication; *b* with sonication. Scan rate 0.1 V s^{-1}

large number of peaks in the whole potential range, *i.e.*, even at potentials where no Faraday current is observed without sonication. This implies that microjets cause a strong increase in the charging current.

2) The shape of individual current peaks is different. At platinum the Faraday current increases rapidly, *i.e.*, in less than 0.5 ms (which is the time

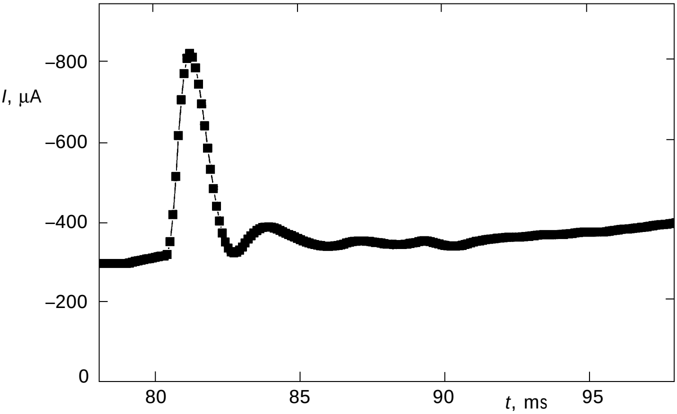

FIG. 5
Shape of an individual current peak at E = –1.13 V (*vs* SCE) recorded at higher time resolution (0.1 ms per point) at mercury pool electrode in aqueous solution of Tl^+ (0.5 mM $TlNO_3$, 0.1 M $KClO_4$)

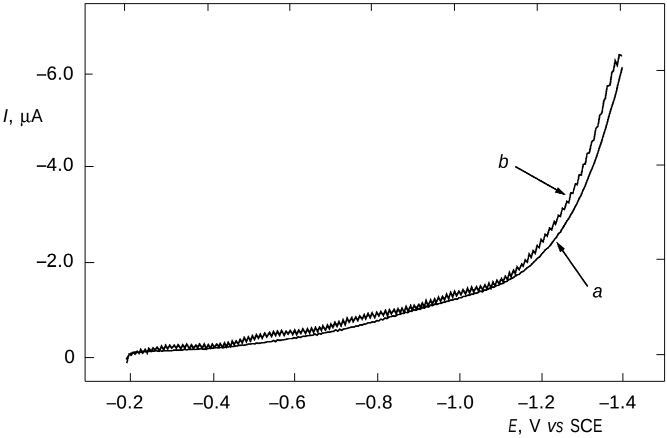

FIG. 6
Voltammograms recorded at platinum disc electrode (surface 0.2 mm^2) in aqueous solution of supporting electrolyte (0.1 M Na_2SO_4): *a* without sonication; *b* with sonication. Scan rate 0.1 V s^{-1}

delay between two recorded points) and, after the rapid increase, the current decreases more slowly. On the other hand, at mercury, the peaks are rather symmetrical: the current first gradually increases within *ca* 0.8 ms, thereafter decreasing back in *ca* 1.3 ms, *i.e.*, with approximately the same rate.

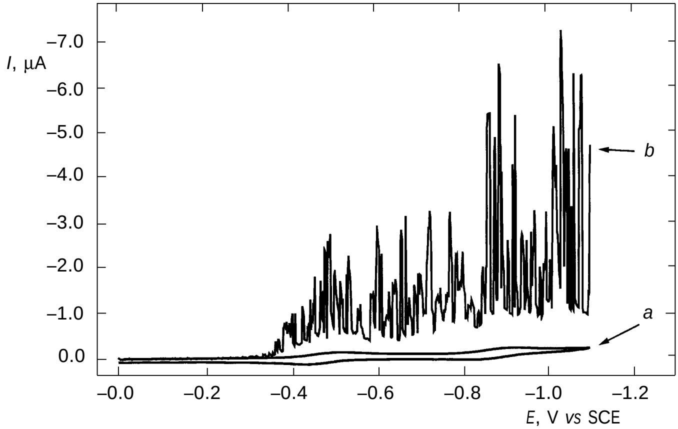

FIG. 7
Voltammograms of methylviologen (0.23 mmol l^{-1}) in acetonitrile/TBAH (0.1 mol l^{-1}) recorded at platinum disc electrode (surface 0.2 mm^2): *a* without sonication; *b* with sonication. Scan rate 0.1 V s^{-1}

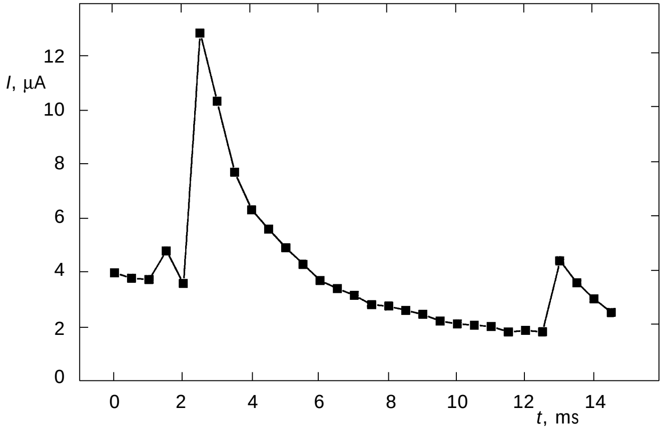

FIG. 8
Shape of an individual current peak recorded at E = –1.0 V (*vs* SCE) at higher time resolution (0.5 ms per point) at platinum disc electrode (surface 0.2 mm^2) for methylviologen (0.23 mmol l^{-1}) in acetonitrile/TBAH (0.1 mol l^{-1})

The increase in the blank current on the mercury pool is evidently caused by microjets: when the jet of liquid hits the surface of mercury, a pressure pulse makes mercury move. A pit in its surface is made and, consequently, the electrode surface becomes larger (Fig. 9). Charging of this new surface is responsible for a current increase. The increasing current is thus a capacity current.

Calculation of the Surface Enlargement Caused by Microjets

A detailed analysis of sonovoltammogram shows a number of peaks of different intensity. It is evident that the peak height is given by the microjet size which depends on the distance of collapsing bubble from the electrode surface. The largest and most intense microjets, corresponding to the highest current peaks, are formed by collapses of bubbles formed directly at the electrode surface.

Integration of the area of such intense peak gives a charge Q_p (which is ca $2.5 \cdot 10^{-7}$ C in the case of a peak formed at *ca* –1.0 V) used for charging the newly formed surface. Integration of the capacity current (recorded without sonication) for charging the whole mercury pool surface area A (*ca* 16 mm^2) to the same potential gives a charge Q_E ($1.9 \cdot 10^{-6}$ C). Hence, the maximum newly formed surface area ΔS created by one jet is given by Eq. (*1*).

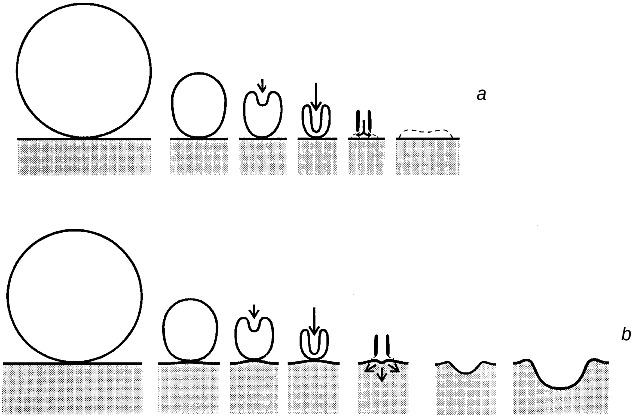

FIG. 9
Expected history of bubble collapsing at the electrode surface: a solid electrode; b mercury pool electrode

$$\Delta S = Q_p/Q_E \cdot A = 0.25/1.9 \cdot 16 = 2.1\ \mathrm{mm}^2 \qquad (1)$$

In the presence of an electroactive solution, the current increase due to sonication is a sum of the increase in the capacity current and of the electrolytic (Faraday) current. The electrolytic current increases due to:

a) the increase in the electrode surface caused by microjetting, and

b) the mass transfer enhancement caused by all the effects mentioned above in the introduction, *i.e.*, acoustic streaming, microstreaming and turbulence (a steady part of the current increase) and microjetting (an oscillatory part of the current).

As can be seen from Fig. 7, the influence of microjetting predominates. This is probably due to a good distribution of ultrasonic intensity within the cell, where a high local intensity is assured in the vicinity of the working electrode, and a cylindrical shape of the cell with a small diameter, which does not enable macroscopic acoustic streaming.

The rate of the current increase in every pulse on the liquid mercury electrode is controlled by the rate of formation of the new surface. Microjet itself, which is an impulse to the motion of the mercury surface, lasts only about 0.7 μs (ref.[9]). However, the motion of mercury and, consequently, the increase in the electrode surface persist a longer time due to inertia of both the solution and mercury.

This is an important difference from the case of electrolytic current at a solid electrode, where all macroscopic motion is stopped soon after the microjet is finished. Consequently, after the rapid increase, the current decreases slowly according to Cotrell law[27] ($I \sim t^{-1/2}$), which means that the current decrease is diffusion-controlled[9].

Diffusion Layer Thickness

In electrochemical processes controlled by mass transport, the concept of diffusion layer thickness, δ, defined by Eq. (*2*) (ref.[27]) applies:

$$(\mathrm{d}c/\mathrm{d}x)_{x=0} \cdot \delta = c_{\mathrm{bulk}} - c_{\mathrm{surface}}\ . \qquad (2)$$

This equation approximates the concentration–electrode distance function, $c(x)$, by a linear dependence. According to this model, the diffusion-controlled current is described by Eq. (*3*):

$$I = \frac{nFDA(c_{\text{bulk}} - c_{\text{surface}})}{\delta}\,, \tag{3}$$

where I is the current, n the number of transferred electrons, F the Faraday constant, D the diffusion coefficient, A the electrode area, c the concentration, and δ the diffusion layer thickness. Experimental values ($n = 1$, $F = 96\,494$ C mol^{-1}, diffusion coefficient of Tl^+ in water[28] $D = 2.00 \cdot 10^{-5}$ cm^2 s^{-1}, $A = 16$ mm^2, $c_{\text{bulk}} = 5 \cdot 10^{-4}$ mol l^{-1}, $c_{\text{surface}} = 0$ mol l^{-1} and $I = 100$ μA) give the thickness of the diffusion layer, δ, of about 16 μm. However, these data describe the average values over the whole electrode surface. As the distribution of current density is very inhomogeneous due to microjets, local values of δ should be considered (Figs 10a–10c).

According to the Eq. (3), when considering the maximum values for the peak current ($I_{\text{peak}} = 400$ μA) and the corresponding newly formed surface (2.1 mm^2), the local value of δ during microjet decreases down to 0.5 μm.

It is evident that for the current increase, which has a local character, mainly microjets are responsible.

Electrode Activation by Sonication

The main advantage of sonication, which is impossible to achieve by other methods, is electrode activation during electrolysis. As example serves electrooxidation of cysteine, demonstrated in Fig. 11.

It is known that anodic oxidation of cysteine in aqueous solution (0.1 M acetate buffer, pH 4.55) at the mercury electrode results in passivation of the electrode surface by adsorption of the product of the electrode reaction, which is cysteine mercurous thiolate[29]. In the course of controlled-potential

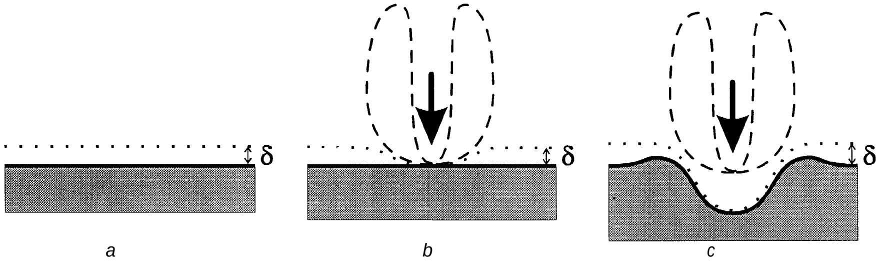

FIG. 10
Profile of the diffusion layer thickness δ during electrolysis: a at solid electrode without sonication; b at sonicated solid electrode; c at sonicated mercury pool electrode

electrolysis, the mercury pool is completely covered by a film of the oxidation product which passivates the electrode in several seconds (curve *a*). Mechanical stirring of the solution has only a limited effect (curve *b*). However, sonication of the electrode results in a dramatic current increase in a number of peaks (curve *c*) due to mechanical removal of the passivating film and/or due to the formation of fresh unpassivated mercury surface.

CONCLUSIONS

Two experimental arrangements for sonoelectrochemical studies at liquid mercury electrodes have been developed and tested.

It was shown that advantages of sonication, *i.e.*, local mass transfer enhancement and electrode surface activation, can be utilized even with mercury pool electrodes.

The current increase was explained by cavitation. Microjets of solution, resulting from asymmetric bubble collapses in the neighbourhood of the electrode, form a new electrode surface and bring the matter from the bulk solution to the electrode. About 2 mm^2 of fresh electrode surface can be formed by one collapsing bubble and the thickness of the diffusion layer can be decreased down to *ca* 0.5 μm.

It was demonstrated that sonication can be used for reactivation of passivated electrode surface during electrolysis.

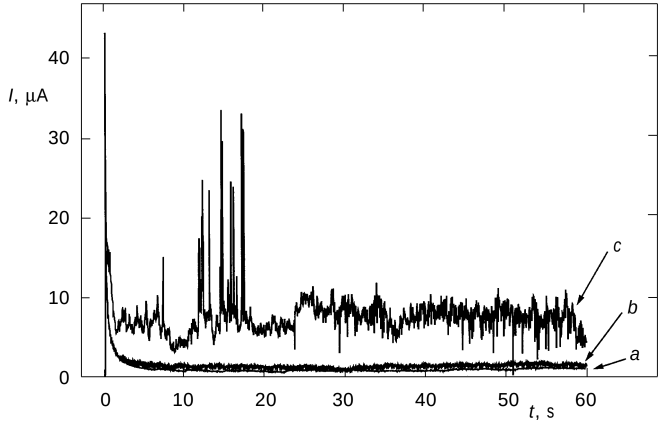

FIG. 11
Electrooxidation of cysteine in aqueous solution (0.1 M acetate buffer, pH 4.55) at mercury pool electrode; E_a = –0.45 V (*vs* SCE): *a* without stirring; *b* with stirring of the solution by inert gas flow; *c* with sonication

This work was supported by the Grant Agency of the Czech Republic (grant No. 203/97/0866).

REFERENCES

1. Walton D. J., Phull S. S. in: *Advances in Sonochemistry* (T. J. Mason, Ed.), Vol. 4. JAI Press, Greenwich 1996.
2. Compton R. C., Eklund J. C., Marken F.: *Electroanalysis* **1997**, *9*, 509.
3. Starritt H. C., Duck F. A., Humprey V. F.: *Ultrasound Med. Biol.* **1989**, *15*, 363.
4. Leighton T. G.: *The Acoustic Bubble*. Academic Press, London 1994.
5. Compton R. G., Eklund J. C., Page S. D., Mason T. J., Walton D. J.: *J. Appl. Electrochem.* **1996**, *26*, 775.
6. Elder S. A.: *J. Acoust. Soc. Am.* **1958**, *31*, 54.
7. Plesset M. S., Chapman R. B.: *J. Fluid Mech.* **1971**, *47*, 283.
8. Klíma J., Bernard C., Degrand C.: *J. Electroanal. Chem.* **1994**, *367*, 297.
9. Klíma J., Bernard C., Degrand C.: *J. Electroanal. Chem.* **1995**, *399*, 147.
10. Compton R. G., Eklund J. C., Page S. D., Sanders G. H. W., Booth J.: *J. Phys. Chem.* **1994**, *98*, 12410.
11. Madigan N. A., Hagan C. R. S., Coury L. A., Jr.: *J. Electrochem. Soc.* **1994**, *141*, L23.
12. Klíma J., Bernard C.: *J. Electroanal. Chem.* **1999**, *462*, 181.
13. Macounová K., Klíma J., Bernard C., Degrand C.: *J. Electroanal. Chem.* **1998**, *457*, 141.
14. Benahcene A., Petrier C., Reverdy G., Labbe P.: *New J. Chem.* **1995**, *19*, 989.
15. Akkermans R. P., Ming W., Bains C. D., Fidel-Suáres M., Compton R. G.: *Electroanalysis* **1998**, *10*, 613.
16. Madigan N. A., Hagan C. R. S., Zhang H., Coury L. A., Jr.: *Ultrasonic Sonoelectrochem.* **1996**, *3*, S239.
17. Atobe M., Nonaka T.: *Bull. Chem. Soc. Jpn.* **1998**, *71*, 397.
18. Atobe M., Matsuda K., Nonaka T.: *Electroanalysis* **1996**, *8*, 784.
19. Mason T. J., Lorimer J. P., Walton D. J.: *Ultrasonics* **1990**, *28*, 333.
20. Novotný L.: *Chem. Listy* **1995**, *89*, 320.
21. Novotný L.: *Collect. Czech. Chem. Commun.* **1996**, *61*, 1703.
22. Lee C.-W., Compton R. G., Eklund J. C., Waller D. N.: *Ultrason. Sonochem.* **1995**, *2*, S59.
23. Agra-Gutiérrez C., Compton R. G.: *Electroanalysis* **1998**, *10*, 603.
24. Matysik F.-M., Matysik S., Oliveira Brett A. M., Brett C. M. A.: *Anal. Chem.* **1997**, *69*, 1651.
25. Klíma J.: Unpublished results.
26. Marken F., Compton R. G.: *Ultrason. Sonochem.* **1996**, *3*, S131.
27. Bard A. J., Faulkner L. R.: *Electrochemical Methods: Fundamentals and Applications*. Wiley, New York 1980.
28. Heyrovský J., Kůta J.: *Principles of Polarography*. Czechoslovak Academy of Sciences, Prague 1965.
29. Heyrovský M., Vavřička S.: *J. Electroanal. Chem.* **1997**, *423*, 125.